


 Cite this: *RSC Adv.*, 2020, 10, 29627

# Extreme enhancement of secondary chirality through coordination-driven steric changes of terpyridyl ligand in glutamide-based molecular gels†

 Makoto Takafuji,<sup>ID</sup>\*<sup>a</sup> Tomoki Kawahara,<sup>a</sup> Nahid Sultana,<sup>a</sup> Naoya Ryu,<sup>ID</sup><sup>b</sup>  
Kyohei Yoshida,<sup>ID</sup><sup>c</sup> Yutaka Kuwahara,<sup>ID</sup><sup>a</sup> Reiko Oda,<sup>ID</sup><sup>c</sup> and Hirota Iihara,<sup>ID</sup>\*<sup>a</sup>

Aggregation-induced chirality is potentially useful in sensor technology applications. Herein we show extreme enhancement of secondary chirality through coordination-driven steric changes of terpyridyl ligand in molecular gels. The secondary chirality reflecting on enhancement of chiral signals (*i.e.*, circular dichroism (CD) and circularly polarised luminescence (CPL)) of the molecular gels formed from glutamide-attached terpyridine (**G-tpy**) is extremely enhanced by the coordination of its terpyridyl groups to metal ions such as Cu<sup>2+</sup>, Zn<sup>2+</sup> and Ru<sup>2+</sup>, which is due to dramatic changes in the stacked structure of the chromophore groups through the formation of metal ion complex. Metal-free terpyridine exists in a non-planar geometry, which suppress  $\pi$ - $\pi$  stacking interactions among aggregates. The planarity of the terpyridyl group is improved through metal-ion complexation, which induces the metal-ion-coordinated terpyridyl groups to stack. The thermal stabilities of the CD signals are strongly affected by the metal-ion species. CPL signal is generated in the molecular gel formed from **G-tpy**-Zn<sup>2+</sup> complex accompanied by chelation-enhanced fluorescence. It is expected that large and sensitive coordination-driven secondary chirality signals (CD and CPL) are useful for sensing guest molecules and the surrounding environment.

Received 8th June 2020

Accepted 3rd August 2020

DOI: 10.1039/d0ra05057a

[rsc.li/rsc-advances](http://rsc.li/rsc-advances)

## Introduction

Organic ligands can be powerful responsive chromophoric tools for metal-ion complexes, as their absorption and emission properties are effectively changed through coordination.<sup>1</sup> In sensors, such changes can be used to detect the nature of the surrounding environment, including temperature, pH, and additives present. A self-assembling system can amplify spectroscopic signals due to dramatic changes in its structural ordering.<sup>2</sup> We reported molecular gel-forming chiral glutamide derivatives with organic ligands.<sup>3</sup> The glutamide unit acts as a molecular tool that chirally orders the chromophoric groups, thereby inducing circularly polarised signals;<sup>4</sup> coordination-complexation with metal ions also

induces remarkable changes in chiroptical properties.<sup>5</sup> The tuneable and sensitive chiroptical properties of these glutamide-attached chromophores (luminophores), such as circular dichroism (CD) and circularly polarised luminescence (CPL), are attractive features. Such chiroptical properties based on self-assembling system are recognized as “supramolecular chirality”.<sup>6</sup> Terpyridyl ligands are broadly used in coordination chemistry because metal complexation strongly enhances its emission signals.<sup>7</sup> Emission enhancement from the terpyridyl group is based on its rigid geometry, with the emission wavelength strongly affected by factors that include the kind of metal ion and the coordination structure. Therefore, various terpyridine complexes with unique luminescence properties are potentially useful in a number of applications, such as chemo-sensing, photocatalysis,<sup>8</sup> detecting biological activity through DNA intercalation<sup>9</sup> and covalent binding to biomolecules, with antitumor, radiotherapy, antiprotozoal agents, and protein probes as possible applications.<sup>10,11</sup> Herein, we report that the secondary chirality of glutamide-attached terpyridine (**G-tpy**, Fig. 1a) self-assemblies arises through coordination with metal ions, which also effectively enhances optical activity. The strategy of this work is schematically illustrated in Fig. 1b.

<sup>a</sup>Department of Applied Chemistry and Biochemistry, Kumamoto University, 2-39-1 Kurokami, Chuo-ku, Kumamoto 860-8555, Japan. E-mail: takafuji@kumamoto-u.ac.jp; iihara@kumamoto-u.ac.jp

<sup>b</sup>Materials Development Department, Kumamoto Industrial Research Institute, 3-11-38 Higashimachi, Higashi-ku, Kumamoto 862-0901, Japan

<sup>c</sup>Institut de Chimie & Biologie des Membranes & des Nano-objets (UMR5248 CBMN), CNRS, Université de Bordeaux, Institut Polytechnique Bordeaux, 2 rue Robert Escarpit, 33607 Pessac, France

† Electronic supplementary information (ESI) available. See DOI: 10.1039/d0ra05057a



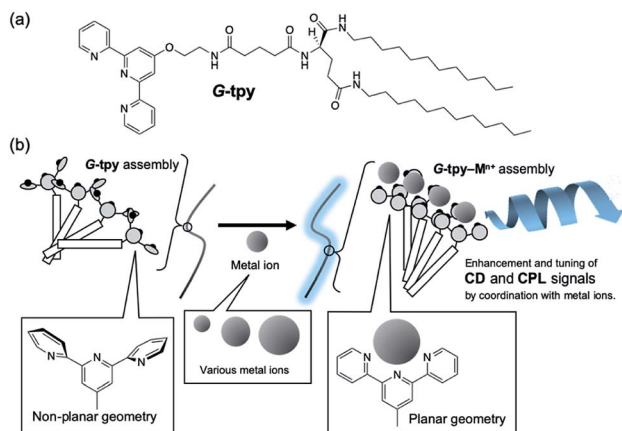


Fig. 1 (a) Chemical structure of the glutamide-attached terpyridine (**G-tpy**), and (b) schematic illustration of the strategy of this work.

## Results and discussion

### Gelation property of **G-tpy**

**G-tpy** was synthesised by the amide coupling reaction of aminopropyl oxy terpyridine<sup>11</sup> with double-alkylated glutamide<sup>12</sup> using diethyl phosphoryl cyanide as a coupling reagent. The terpyridyl ligand was connected to the self-assembling molecular tool (**G**) via a flexible ether linker. The solubility of **G-tpy** was examined in a variety of organic solvents and their mixtures (Table S1†). Since **G-tpy** formed an organogel in a 9 : 1 mixture of cyclohexane–ethanol at ambient temperature (Fig. S1†), this mixture was chosen as the solvent for investigating **G-tpy** self-assembly in the absence and presence of metal ions.

### Effect of metal ions on the secondary chirality of **G-tpy**

Absorption spectra of chiral ligand **G-tpy** and their metal complexes with  $\text{Cu}^{2+}$ ,  $\text{Zn}^{2+}$  and  $\text{Ru}^{3+}$  in the mixed solvent of cyclohexane and ethanol (9 : 1) were investigated. Two absorption bands were recorded at about 240 and 280 nm from  $\pi$ – $\pi^*$  intraligand charge transfer transition of **G-tpy**.<sup>13</sup> The peaks red shifted to 326 nm, 316 nm and 395 nm by addition of  $\text{Cu}^{2+}$ ,  $\text{Zn}^{2+}$  and  $\text{Ru}^{3+}$  respectively (Fig. S2†), indicating that the formation of metal ion-coordinated terpyridyl group. This is associated due to the metal to ligand charge transfer transition. Similar spectral changes have been reported for the terpyridine derivatives through the complexation with metal ions.<sup>14</sup> The absorption of each system at 320 nm as a function of metal-ion concentration is shown in Fig. S2d,† which reveals that **G-tpy** self-assembles form 2 : 1 complexes with the metal ions examined in this study. Strong circular dichroism (CD) signals are induced around the absorption band of the terpyridyl moiety by the addition of metal ions at concentration ratios of 2 : 1 and 1 : 1 (Fig. S3†). In this study we spectroscopically and microscopically examined **G-tpy** solutions with 1.0 molar equivalent of metal ions ( $[\text{G-tpy}]/[\text{metal ion}] = 1 : 1$ ). CD enhancement is generally observed in self-assembled **G** molecules that contain chromophores; this phenomenon is referred to as “secondary chirality” and is based on the supramolecular chirality of the

chromophores in the self-assembly. For instance, a **G**-attached pyrene as the chromophore (**G-pyr**,<sup>3c</sup> Fig. S4†) shows a comparably large CD signal around its absorption band; **G-pyr**:  $[\theta]_{325} = -4.1 \times 10^5 \text{ cm}^2 \text{ dmol}^{-1} \text{ L}^{-1}$ ,  $[\theta]_{355} = 10.7 \times 10^5 \text{ cm}^2 \text{ dmol}^{-1} \text{ L}^{-1}$ . In comparison, almost no CD signals are observed for **G-tpy** in the absence of metal ions, which is due to the non-planar geometry of the terpyridyl moiety that prevents the spatial chiral arrangement. Interestingly the spectral pattern and the CD intensity of **G-tpy** are strongly affected by the metal-ion species (Fig. 2a). The addition of 0.5 molar equivalents of  $\text{Cu}^{2+}$  induces positive and negative CD signals at around 323 and 276 nm, respectively. A similar CD pattern is observed for **G-tpy** in the presence of  $\text{Ru}^{3+}$ , but with extremely large molecular ellipticities. In comparison, the opposite CD pattern is observed for **G-tpy** complexed with  $\text{Zn}^{2+}$ , with negative and positive signals at around 291 and 312 nm respectively. The molecular ellipticities of the CD signals obtained from **G-tpy** in the presence of  $\text{Zn}^{2+}$  and  $\text{Ru}^{3+}$  are of the order of  $10^5$ , which is relatively large. Similar changes have been reported for organic–ligand-functionalised **G** through complex formation with metal ions. For instance, the CD signals of **G**-attached isoquinoline (**G-iq**, Fig. S4†) shows induced CD signals at 258 and 290 nm, and these signals change upon the addition of metal ions, such as  $\text{Cu}^{2+}$ ,  $\text{Zn}^{2+}$  and  $\text{Co}^{2+}$ .<sup>5a</sup> The spectral patterns of **G-iq** in the presence and absence of a metal ion are completely different and depend on the metal-ion species. For instance,  $\text{Cu}^{2+}$  induces a redshift accompanied by a sign-reversed CD signal from the **G-iq**. The observed intensities of the CD signals without and with  $\text{Cu}^{2+}$  are similar. In comparison,  $\text{Co}^{2+}$  reduces

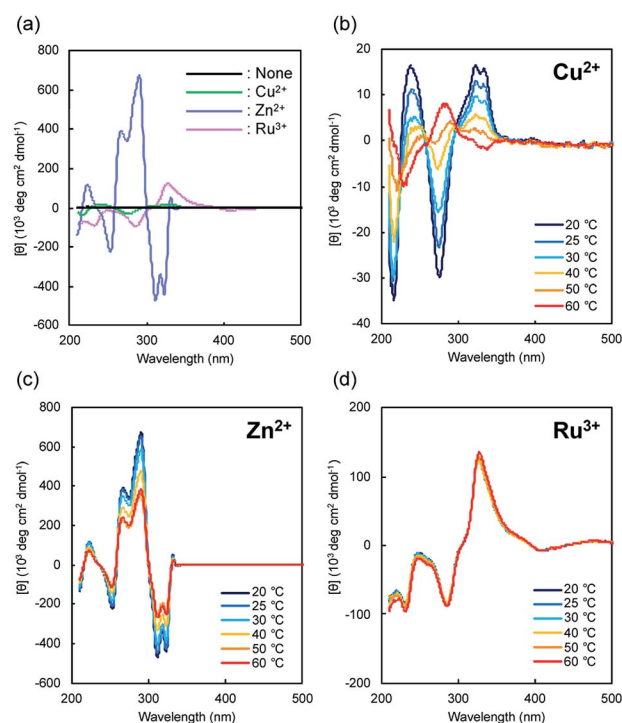


Fig. 2 (a) CD spectra of **G-tpy** without and with metal ions. (b–d) Temperature dependencies of CD spectra with metal ions.  $[\text{G-tpy}] = 0.5 \text{ mM}$ ,  $[\text{metal ion}] = 0.5 \text{ mM}$ .

the intensities of the CD signals of **G-tpy** and the geometry of the isoquinoyl group is almost unchanged after coordination with the metal ion.

As discussed above, remarkable CD-signal enhancements from **G-tpy** are observed after coordination to a metal ion, which are due to dramatic changes in the stacked structure of the chromophore groups through complexation to the metal ion. Metal-free terpyridine exists in a non-planar geometry,<sup>15</sup> which suppress  $\pi$ - $\pi$  stacking interactions among aggregates. The planarity of the terpyridyl group is improved through metal-ion complexation, which induces the metal-ion-coordinated terpyridyl groups to stack. The single-crystal X-ray diffraction analysis has been applied to confirm the steric geometry of pyridine rings in a crystal state of terpyridyl derivatives without and with transition metal ions such as  $\text{Fe}^{3+}$ ,<sup>16a</sup>  $\text{Pd}^{2+}$ ,<sup>16b</sup>  $\text{Co}^{2+}$ ,<sup>16c</sup> and  $\text{Zn}^{2+}$ .<sup>16c</sup> In most of the cases, the free terpyridine form a transoid (*trans-trans*) arrangement,<sup>17</sup> whereas the complex become in a square planar geometry after coordination with metal ion. It is important that the planarity of terpyridine-metal ion complex depend on the parameters of metal ions such as size and the coordination number.<sup>16</sup> <sup>1</sup>H NMR spectroscopies of **G-tpy** in a mixture of cyclohexane-*d*<sub>12</sub> and ethanol-*d*<sub>6</sub> (9 : 1) revealed that the peaks of terpyridyl group were broadened by addition of equivalent of metal ions (Fig. S5†). It was considered that the molecular orientation of **G-tpy** changed dramatically by coordination with metal ions, however the geometric changes of the pyridyl group could not be confirmed by the 2D NMR. Significant CD-signal enhancement is the result of the spatial chiral arrangement of the planar metal-ion-coordinated terpyridyl group of **G-tpy**. Since no low energy absorption bands are observed, ligand-to-metal charge transfer appears not to occur.<sup>18</sup> Interestingly the thermal responsiveness of the induced CD signals of **G-tpy** depends on the metal-ion species. Fig. 2 shows the CD spectra of **G-tpy**- $\text{Cu}^{2+}$  (b), **G-tpy**- $\text{Zn}^{2+}$  (c), **G-tpy**- $\text{Ru}^{3+}$  (d) over a wide range of temperatures (20–60 °C). The **G-tpy**- $\text{Cu}^{2+}$  complex shows CD signals that sign-reverse upon heating, from positive ( $[\theta]_{323} = 16.4 \times 10^3 \text{ deg cm}^2 \text{ dmol}^{-1}$ ) to negative ( $[\theta]_{323} = -0.5 \times 10^3 \text{ deg cm}^2 \text{ dmol}^{-1}$ ) at 323 nm, and from negative ( $[\theta]_{276} = -29.8 \times 10^3 \text{ deg cm}^2 \text{ dmol}^{-1}$ ) to positive ( $[\theta]_{276} = 7.0 \times 10^3 \text{ deg cm}^2 \text{ dmol}^{-1}$ ) at 276 nm. Similar CD-inversion trends were reported for complexes of terpyridyl-based ligands connecting alanine moieties, in which chirality could be controlled by the relative proportion of the terpyridyl derivative and its Pt complex.<sup>19</sup> The induced CD signals are somewhat more thermally stable in **G-tpy** through complexation with  $\text{Zn}^{2+}$  and  $\text{Ru}^{3+}$ ; in **G-tpy**- $\text{Ru}^{3+}$  they showed almost no change in the 20–60 °C temperature range.

Differential scanning calorimetry (DSC) was used to observe the gel-to-sol phase transitions of **G-tpy** in the absence and presence of metal ions. Because of the small enthalpies associated with phase transitions, somewhat higher concentrations (10 mM in a 9 : 1 mixture of cyclohexane-ethanol) of **G-tpy** were used. As shown in Fig. S6,† a remarkably small endothermic peak ( $\Delta H = 0.5 \text{ kJ mol}^{-1}$ ) with a maximum at 65 °C was observed for the **G-tpy** solution devoid of metal ions. In comparison, lower endothermic peaks (38 °C and 51 °C) were observed for **G-tpy** with 0.5 equivalents of  $\text{Cu}^{2+}$  and  $\text{Zn}^{2+}$ ,

respectively (**G-tpy** precipitates from solution upon addition of 0.5 equivalents of  $\text{Ru}^{3+}$ ), and was accompanied by increases in the phase-transition enthalpy ( $\Delta H = 1.08$  and  $4.07 \text{ kJ mol}^{-1}$ , respectively). These results indicate that coordination induces the rearrangement of the molecular orientation of **G-tpy** accompanied with chiral stacking of terpyridyl groups. The heat sensitivity of the ordering structure of **G-tpy** is depend on the metal ion species, particularly the **G-tpy**- $\text{Cu}^{2+}$  complex is sensitive to heat.

#### Aggregation morphology of **G-tpy** molecular gel with metal ion

Rearrangement of the molecular orientation through the formation of a metal-ion complex is often accompanied by a morphological transformation. The **G-tpy** formed nano-fibrillar aggregates in 9 : 1 cyclohexane-ethanol solution and transformed into fragmented ribbons and tape-like structures in the presence of  $\text{Co}^{2+}$  and  $\text{Cu}^{2+}$ , respectively.<sup>5a</sup> **G-tpy** also formed 7 nm diameter nano-fibrous aggregates, and showed no drastic changes in morphological features upon addition of 1.0 equivalents of  $\text{Cu}^{2+}$ ,  $\text{Zn}^{2+}$ , or  $\text{Ru}^{3+}$  (Fig. 3), irrespective of the remarkable changes observed by CD spectroscopy. It was confirmed that the fibrous aggregates of **G-tpy**- $\text{Zn}^{2+}$  complex bundled into a larger aggregate. Similar bundled structure is often observed in the self-assemblies, which induce the 3 dimensional structure to form gel. Further investigates are needed to clarify the relevance of aggregation structure and exceptional large CD and fluorescence signals in **G-tpy**- $\text{Zn}^{2+}$  complex.

#### Coordination-induced circularly polarized luminescence

The blue coloured emission from **G-tpy** under UV light (365 nm) is affected by the addition of the metal ion; the emission from self-assembled **G-tpy** is quenched by  $\text{Cu}^{2+}$  and  $\text{Ru}^{3+}$ , but is enhanced by  $\text{Zn}^{2+}$  (Fig. 4a). Fluorescence spectra acquired by excitation at 320 nm confirm that the intensity of the fluorescence emitted by **G-tpy** increased significantly upon addition of  $\text{Zn}^{2+}$  (Fig. 4b) and was almost saturated in the presence of 0.5 equivalents of  $\text{Zn}^{2+}$ , which indicates that fluorescence is also

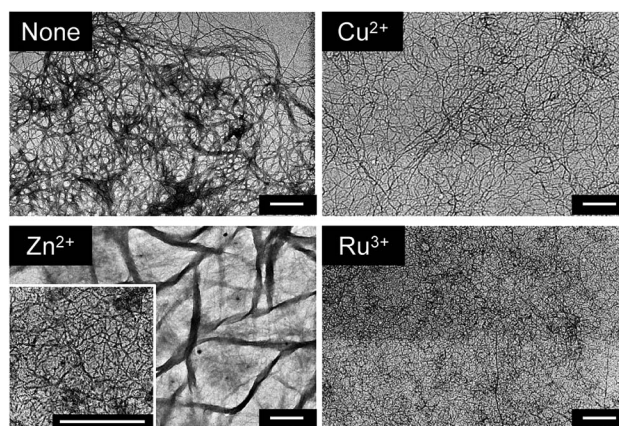


Fig. 3 TEM images of **G-tpy** without and with metal ions. [**G-tpy**] = 0.5 mM, [metal ion] = 0.5 mM. The scale bars indicate 500 nm.



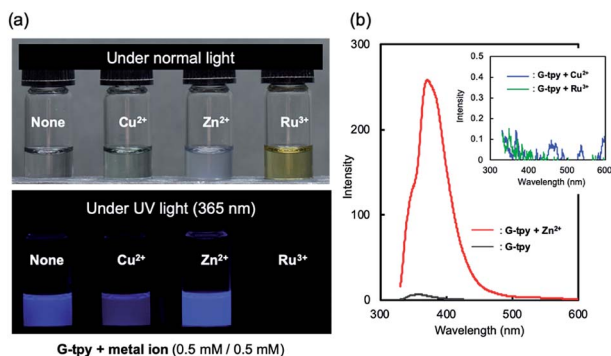


Fig. 4 (a) Photographic images of *G*-tpy solutions without and with various metal ions under normal and UV light (365 nm). (b) Fluorescence spectra of *G*-tpy in the presence of Zn<sup>2+</sup>, Cu<sup>2+</sup>, and Ru<sup>3+</sup>. Solvent: cyclohexane–ethanol (9 : 1). [*G*-tpy] = 0.5 mM, [metal ion] = 0.5 mM.

enhanced through the formation of a 1 : 2 complex with Zn<sup>2+</sup> (Fig. S7†). Fluorescence signal is remarkably decreased when *G*-tpy self-assembles with equimolar of Cu<sup>2+</sup> or Ru<sup>3+</sup> (Fig. 4b). Similar chelation-enhanced fluorescence (CHEF) and chelation-quenched fluorescence (CHQF) have been reported for phenylenevinylene terpyridine chelated with Cd<sup>2+</sup> and Zn<sup>2+</sup>, in which the planarity of the terpyridyl moiety influences emission behavior.<sup>20</sup> The complex formed between the terpyridyl group and each metal ion is expected to be complicated due to perturbations from the highly oriented structure of the *G* moiety. Further investigations are needed in order to clarify the CHEF and CHQF mechanisms involved in *G*-tpy self-assembly; however, such phenomena are useful for sensor applications despite the absence of mechanistic details. An extremely enhanced CD signal as well as fluorescence emission was observed for the *G*-tpy–Zn<sup>2+</sup> self-assembled structure; therefore *G*-tpy–Zn<sup>2+</sup> was examined by CPL spectroscopy. The spectra in Fig. 5 reveals a CPL signal at around the emission wavelength of *G*-tpy–Zn<sup>2+</sup>, in which the CPL and fluorescence intensities are changed simultaneously depending on the excitation wavelength. The CPL dissymmetry factor ( $|g_{\text{lum}}|$ ) of *G*-tpy–Zn<sup>2+</sup> (Ex. = 310 nm) was calculated to be  $1.7 \times 10^{-3}$  (at 364.5 nm), which is not surprisingly large and commonly obtained for *G*-attached

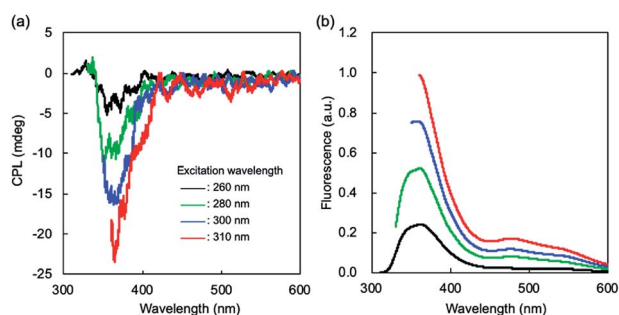


Fig. 5 (a) CPL and (b) fluorescence spectra of *G*-tpy solutions without and with Zn<sup>2+</sup>. [*G*-tpy] = 0.5 mM. [Zn<sup>2+</sup>] = 0.5 mM. Solvent: cyclohexane–ethanol (9 : 1).

chromophores.<sup>4</sup> Almost no CPL signal was observed for *G*-tpy alone, nor its metal ion complexes with Cu<sup>2+</sup> or Ru<sup>3+</sup> (Fig. S8†).

## Experimental

### Synthesis of *G*-tpy

**Materials.** All chemicals used for synthesis of *G*-tpy in this study were of analytical grade and were used as received without any further purification.

**Synthetic procedure of *G*-tpy.** The synthetic scheme for *G*-tpy is depicted in Fig. S9.† *N*<sup>1</sup>-4-carboxybutanoyl-*N*<sup>2</sup>,*N*<sup>3</sup>-didodecyl-L-glutamide (*G*-COOH) was synthesized according to our previous report,<sup>21</sup> and 4'-chloro-2,2':6',2''-terpyridine (tpy-NH<sub>2</sub>) was synthesized according to the literature.<sup>11</sup> The details of synthesis are described in the ESI† and the chemical structures were characterized by elemental analysis (Micro Coder JM10, J-Science Lab Co., Ltd., Kyoto, Japan), FT-IR (FT/IR4100 spectrophotometer, JASCO Co., Tokyo, Japan) and <sup>1</sup>H NMR (JNM-ECZ400R NMR spectrometer, JEOL Ltd., Tokyo, Japan) spectroscopies. *G*-COOH (0.40 g, 0.67 mmol), tpy-NH<sub>2</sub> (0.23 g 0.79 mmol), triethylamine (TEA, 2.53 g 3.48 mmol) and diethyl cyanophosphonate (DEPC, 0.45 mL 2.88 mmol) were dissolved in chloroform (200 mL) and the mixture was stirred for 1 hour in the ice water. Then the reaction mixture was stirred for 1 day in the room temperature. The reaction mixture was washed with 0.3 N HCl (3×), 1 N NaOH (3×) and water (3×). The chloroform solution was dried over Na<sub>2</sub>SO<sub>4</sub> and the solvent was removed. After it was recrystallized by methanol to give a white powder: yield 464 mg (80%).

**Identification of *G*-tpy.** Mp 192.0–196.0 °C. IR spectrum (KBr): 3292, 2920, 2850, 1637, 1556, 1204 cm<sup>-1</sup>. <sup>1</sup>H NMR (400 MHz, CDCl<sub>3</sub>, TMS, 25 °C): δ 0.86–0.90 (t, 6H, –CH<sub>3</sub>), 1.25–1.30 (m, 36H, –(CH<sub>2</sub>)<sub>9</sub>–), 1.45–1.52 (m, 4H, –NHCH<sub>2</sub>CH<sub>2</sub>–), 1.90–2.01 (m, 2H, –C\*HCH<sub>2</sub>–) 1.97–2.01 (t, 2H, –C\*HNHC(=O)CH<sub>2</sub>CH<sub>2</sub>–), 2.30–2.39 (m, 6H, –CH<sub>2</sub>CH<sub>2</sub>CH<sub>2</sub>C(=O)–) 3.15–3.25 (dt, 4H, –CH<sub>2</sub>–) 3.66–3.86 (m, 2H, –C\*H NHC(=O)CH<sub>2</sub>CH<sub>2</sub>CH<sub>2</sub>C(=O)NHCH<sub>2</sub>–) 4.32–4.50 (m, 3H, –C\*HNHC(=O)CH<sub>2</sub>CH<sub>2</sub>CH<sub>2</sub>C(=O)NHCH<sub>2</sub>CH<sub>2</sub>–) 6.10–6.15 (t, 1H, –NH–) 6.63–6.72 (t, 1H, –NH–) 6.89–6.97 (d, 2H, –NH–) 7.32–7.35 (t, 2H, H5, 5'') 7.83–7.88 (t, 2H, H4, 4'') 8.03–8.05 (s, 2H, H3', 5') 8.61–8.63 (d, 2H, H3, 3'') 8.68–8.70 (d, 2H, H6, 6''). Anal. calcd for C<sub>34</sub>H<sub>65</sub>N<sub>3</sub>O<sub>5</sub>: C, 70.4; H, 9.2; N, 11.3. Found: C, 70.0; H, 9.7; N, 11.3.

### Methods

**Preparation of the *G*-tpy solution without and with metal ions.** *G*-tpy was dissolved in organic solvent at 70 °C for 5 min, and cooled at ambient temperature. The gelation property of *G*-tpy was confirmed with various organic solvents listed in Table S1† at the concentration of 5 mM at 10 and 70 °C. The spectroscopic measurements, microscopic observations and thermal analysis of *G*-tpy aggregates without and with metal ions were carried out in the mixed solvent of cyclohexane and ethanol (9 : 1). The ethanol solution of metal ion (10 μL) was added to the cyclohexane–ethanol solution of *G*-tpy (1 mL), and the mixture was heated at 70 °C for 5 min, and cooled at 10 °C for 24 h.

**Spectroscopic measurements.** All spectroscopic measurements were carried out in a quartz-cell using the spectrophotometric grade solvents. UV-vis, fluorescence, CD and CPL spectroscopies of **G-tpy** solutions without and with metal ions were measured using V-560, FL-6500, J-725 and CPL-300 (JASCO Co., Tokyo, Japan) respectively.

**Microscopic observations.** The **G-tpy** solution was dropped on the carbon-deposited poly(vinyl formal)-coated copper grid and dried at 25 °C. Uranyl acetate solution was used for staining **G-tpy** aggregates, but no staining reagent was used for **G-tpy**-metal ion complexes. Transmission electron microscopic observations were performed with JEM-1400Plus (JEOL Ltd., Tokyo, Japan).

**Thermal analysis.** The **G-tpy** solution was put in 70 µL Ag cell and sealed tightly. Differential scanning calorimetry was performed using DSC thermal analysis system (DSC7000X, Hitachi High-Tech Science Co., Tokyo, Japan) under nitrogen atmosphere.

## Conclusions

In summary, the secondary chirality of **G-tpy** is extremely enhanced by the coordination of its terpyridyl groups to metal ions. The induced CD signals of **G-tpy** are significantly increased, and the thermal stabilities of the CD signals are strongly affected by the metal-ion species, and CPL signal is generated accompanied by CHEF through the coordination with Zn<sup>2+</sup>. A large and sensitive CD and CPL signal are useful for sensing guest molecules and the surrounding environment. We reported that **G**-attached porphyrine (**G-por**, Fig. S4†) self-assembled with a metal ion can detect pyridine derivatives with various substituents through complexation to the empty site of the metal complex.<sup>5d</sup> We expect that aggregation-induced chiral signals are potentially applicable to sensor technology because they are responsive to multiple stimuli, such as metal ions and temperature. We are currently systematically studying the effects of various metal ions in order to understand the effects of the steric nature of the terpyridyl structure and the orientation of the **G-tpy** structure on enhancing and quenching coordination-driven secondary chirality. Further studies are needed to discuss on the remarkable enhancement of chiroptical properties of **G-tpy** through the coordination with metal ions with nonlinear optical properties such as hyperpolarizability and dipole moment.<sup>22</sup>

## Conflicts of interest

There are no conflicts to declare.

## Acknowledgements

This work is supported by Bilateral Joint Research Projects supported by the Japan Society for the Promotion of Science (JSPS), and Fund for the Promotion of Joint International Research by JSPS.

## Notes and references

- (a) D. R. McMillin and J. Moore, *Coord. Chem. Rev.*, 2002, **229**, 113; (b) U. S. Schubert, H. Hofmeier and G. R. Newkome, *Modern Terpyridine Chemistry*, WILEY-VCH Verlag GmbH & Co. KGaA, 2006.
- I. Eryazici, C. N. Moorefield and G. R. Newkome, *Chem. Rev.*, 2008, **108**, 1834.
- (a) M. Takafuji, H. Ihara, C. Hirayama, H. Hachisako and K. Yamada, *Liq. Cryst.*, 1995, **18**, 97; (b) H. Ihara, H. Hachisako, C. Hirayama and K. Yamada, *J. Chem. Soc., Chem. Commun.*, 1992, **17**, 1244; (c) T. Sagawa, S. Fukugawa, T. Yamada and H. Ihara, *Langmuir*, 2002, **18**, 7223; (d) M. Takafuji, A. Ishiodori, T. Yamada, T. Sakurai and H. Ihara, *Chem. Commun.*, 2004, 1122.
- (a) T. Goto, Y. Okazaki, M. Ueki, Y. Kuwahara, M. Takafuji, R. Oda and H. Ihara, *Angew. Chem., Int. Ed.*, 2017, **56**, 2989; (b) H. Jintoku, M. Kao, A. D. Guerzo, M. Dateki, Y. Yoshigashima, T. Masunaga, M. Takafuji and H. Ihara, *J. Mater. Chem. C*, 2015, **3**, 5970; (c) H. Oishi, K. Yoshida, Y. Kuwahara, M. Takafuji, R. Oda and H. Ihara, *J. Taiwan Inst. Chem. Eng.*, 2018, **92**, 58.
- (a) H. Ihara, T. Sakurai, T. Yamada, T. Hashimoto, M. Takafuji, T. Sagawa and H. Hachisako, *Langmuir*, 2002, **18**, 7120; (b) H. Jintoku, T. Sagawa, M. Takafuji and H. Ihara, *Chem.-Eur. J.*, 2011, **17**, 11628; (c) H. Jintoku, T. Sagawa, T. Sawada, M. Takafuji, H. Hachisako and H. Ihara, *Tetrahedron Lett.*, 2008, **49**, 3987; (d) H. Jintoku, T. Sagawa, M. Takafuji and H. Ihara, *Org. Biomol. Chem.*, 2009, **7**, 2430.
- (a) P. Duan, H. Cao, L. Zhang and M. Liu, *Soft Matter*, 2014, **10**, 5428; (b) T. Shimizu, M. Masuda and H. Minamikawa, *Chem. Rev.*, 2005, **105**, 1401; (c) M. Liu, L. Zhang and T. Wang, *Chem. Rev.*, 2015, **115**, 7304.
- (a) V. M. Suresh, A. De and T. K. Maji, *Chem. Commun.*, 2015, **51**, 14678; (b) G. Barone, A. G. Gennaro, A. M. Giuliania and M. Giustini, *RSC Adv.*, 2016, **6**, 4936; (c) P. Chen, Q. Li, S. Grindy and N. Holten-Andersen, *J. Am. Chem. Soc.*, 2015, **137**, 11590.
- (a) T. J. Wadas, Q. M. Wang, Y. J. Kim, C. Flaschenreim, T. N. Blanton and R. Eisenberg, *J. Am. Chem. Soc.*, 2004, **126**, 16841; (b) C. L. Exstrom, J. R. Sowa, C. A. Daws, D. Janzen, K. R. Mann, G. A. Moore and F. F. Stewart, *Chem. Mater.*, 1995, **7**, 15; (c) C. A. Daws, C. L. Exstrom, J. R. Sowa and K. R. Mann, *Chem. Mater.*, 1997, **9**, 363; (d) W. S. Tang, X. X. Lu, K. M. C. Wong and V. W. W. Yam, *J. Mater. Chem.*, 2005, **15**, 2714; (e) P. W. Du, J. Schneider, P. Jarosz and R. Eisenberg, *J. Am. Chem. Soc.*, 2006, **128**, 7726; (f) M. Cortes, J. T. Carney, J. D. Oppenheimer, K. E. Downey and S. D. Cummings, *Inorg. Chim. Acta*, 2002, **333**, 148.
- (a) K. W. Jennette, S. J. Lippard, G. A. Vassiliades and W. R. Bauer, *Proc. Natl. Acad. Sci. U. S. A.*, 1974, **71**, 3839; (b) S. J. Lippard, *Acc. Chem. Res.*, 1978, **11**, 211; (c) W. D. McFadyen, L. P. G. Wakelin, I. A. G. Roos and B. L. Hillcoat, *Biochem. J.*, 1987, **242**, 177; (d) T. Ihara,

- H. Ohura, C. Shirahama, T. Furuzono, H. Shimada, H. Matsuura and Y. Kitamura, *Nat. Commun.*, 2015, **6**, 6640.
- 10 (a) D. L. Ma, T. Y. T. Shum, F. Y. Zhang, C. M. Che and M. S. Yang, *Chem. Commun.*, 2005, **46**, 75; (b) C. Le Sech, K. Takakura, C. Saint-Marc, H. Frohlich, M. Charlier, N. Usami and K. Kobayashi, *Radiat. Res.*, 2000, **153**, 454; (c) S. Bonse, J. M. Richards, S. A. Ross, G. Lowe and R. L. Krauth-Siegel, *J. Med. Chem.*, 2000, **43**, 4812; (d) E. M. A. Ratilla and N. M. Kostić, *J. Am. Chem. Soc.*, 1988, **110**, 4427.
- 11 G. Maayan, B. Yoo and K. Kirshenbaum, *Tetrahedron Lett.*, 2008, **49**, 335.
- 12 (a) Y. Kira, Y. Okazaki, T. Sawada, M. Takafuji and H. Ihara, *Amino Acids*, 2010, **39**, 587; (b) V. Gopal, J. Xavier, M. Z. Kamal, S. Govindarajan, M. Takafuji, S. Soga, T. Ueno, H. Ihara and N. M. Rao, *Bioconjugate Chem.*, 2011, **22**, 2244.
- 13 (a) S. Gama, I. Rodrigues, F. Marques, E. Palma, I. Correia, M. F. N. Carvalho, J. C. Pessoa, A. Cruz, S. Mendo, I. C. Santos, F. Mendes, I. Santos and A. Paulo, *RSC Adv.*, 2014, **4**, 61363; (b) S. Kuyuldar, C. Burda and W. B. Connick, *RSC Adv.*, 2019, **9**, 21116.
- 14 A. K. Pal, B. Larame-Milette and G. S. Hanan, *Inorg. Chim. Acta*, 2014, **418**, 15.
- 15 (a) S. Y. leung, K. M. Wong and V. W. Yam, *Proc. Natl. Acad. Sci. U. S. A.*, 2016, **113**, 2845; (b) S. Bhowmik, B. Ghosh and K. Rissanen, *Org. Biomol. Chem.*, 2014, **12**, 8836.
- 16 (a) E. C. Constable, G. Zhang, C. E. Housecroft and M. Neuburger, *Inorg. Chem. Commun.*, 2010, **13**, 878; (b) F. Darabi, H. Hadadzadeh, J. Simpson and A. Shahpiri, *New J. Chem.*, 2016, **11**, 9081; (c) B. Whittle, E. L. Horwood, L. H. Rees, S. R. Batten, J. C. Jeffery and M. D. Ward, *Polyhedron*, 1998, **17**, 373.
- 17 (a) A. Anthonysamy, S. Balasubramanian, V. Shanmugaiah and N. Mathivanan, *Dalton Trans.*, 2008, 2136; (b) R. Fallahpour, M. Neuburger and M. Zehnder, *New J. Chem.*, 1999, **23**, 53.
- 18 R. Ziessel, S. Diring and P. Retailleau, *Dalton Trans.*, 2006, 3285.
- 19 K. Kim, J. Kim, C. Moon, J. Liu, S. Lee, M. Choi, C. Feng and J. Jung, *Angew. Chem., Int. Ed.*, 2019, **58**, 11709.
- 20 Z. Zhang, C. Wang, Z. Zhang, Y. Luo, S. Sun and G. Zhang, *Spectrochim. Acta, Part A*, 2019, **209**, 40.
- 21 (a) H. Ihara, M. Takafuji, C. Hirayama and D. F. O'Brien, *Langmuir*, 1992, **8**, 1548; (b) H. Hachisako, Y. Murata and H. Ihara, *J. Chem. Soc., Perkin Trans. 1*, 1999, **2**, 2569; (c) M. Takafuji, H. Ihara, C. Hirayama, H. Hachisako and K. Yamada, *Liq. Cryst.*, 1995, **18**, 97.
- 22 (a) F. Tessore, D. Roberto, R. Ugo and M. Pizzotti, *Inorg. Chem.*, 2005, **44**, 8969; (b) S. K. Peter, C. Kaulen, A. Hoffman, W. Ogieglo, S. Karthaus, M. Homberger, S. Herrero-Pawlis and U. Simon, *J. Phys. Chem. C*, 2019, **123**, 6537.